ChemPubSoc Europe

DOI: 10.1002/chem.201501198

CHEMISTRY
A European Journal
Communication

Protein Folding

Can Helical Peptides Unwind One Turn at a Time? - Controlled Conformational Transitions in α,β^{2,3}-Hybrid Peptides

Dhayalan Balamurugan and Kannoth M. Muraleedharan*[a]

Abstract: Unfolding of helical *trans*-β^{2,3}-hybrid peptides with $(\alpha\text{–}\beta)_n\alpha$ composition, when executed by increasing solvent polarity or temperature, proceeded in a systematic manner with the turns unwinding sequentially; C-terminal region of these peptides were first to unwind and the process propagated towards N terminus with more and more β residues equilibrating from the *gauche* to the *anti* rotameric state across C_α–C_β. This is evidenced by clear change in their C_βH signal splitting, $^3J_{C\alpha H-C\beta H}$ values, and sequential disappearance of *i*,*i*+2 NOEs.

Efforts over the past couple of decades have unraveled the ability of β- and γ-amino acids to assume biologically relevant conformations, such as helix, strand, and turns.[1] Incorporation of natural α-amino acids in the design has not only increased their structural diversity but also has paved way for the development of hybrid systems capable of targeting specific biomolecular recognition events.[2] Results accumulated during these years tend to show many parallels in the folding behavior of synthetic and natural peptides, which gives confidence in using them as models to understand how solvation, secondary interactions, and entropy act in concert during folding and unfolding processes.[3] Folding can be viewed as a cooperative process, during which the energy advantage through intramolecular secondary interactions makes corrections for the loss in entropy.[4] In the case of short helices, folding/unfolding, in principle, can happen step-wise or as a single event. Because the time scales in which the transitions happen are fast, it may be difficult to get a closer look at these processes. However, if the torsions accessible to the amino acid residues are restricted through steric and/or electronic factors, one could expect stabilization of partially folded conformations and a control over their transitions. Results along these lines from our studies on a selected group of *trans*-β^{2,3}-hybrid peptides are discussed below.

Our previous efforts revealed the ability of *trans*-β^{2,3}-amino acid residues to choose a *gauche* conformation across C_α–C_β in response to intramolecular hydrogen bonding, and facilitate 11-helical conformation in their 1:1 hybrids with α-aminoisobutyric acid (Aib); the latter is a known promoter of helical structures in peptides.[1,5] Since these building-blocks have an intermediate flexibility compared to pre-organized (e.g., cyclopentane amino carboxylic acid) and α,β-unsubstituted building-blocks, we expected their peptides to be useful in studying partially folded structures. Initially, we looked at the conformational preferences of oligomers **1**–**4** with $(\alpha\text{–}\beta)_n\alpha$ composition (Figure 1); previous literature reports as well as results from

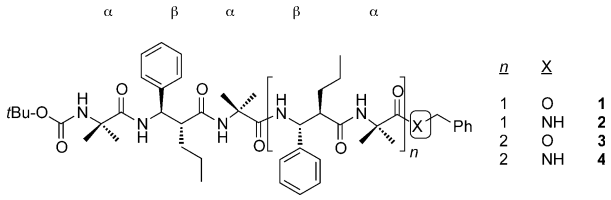

Figure 1. Chemical structures of α,β-hybrid peptide benzyl esters **1** and **3** and benzyl amides **2** and **4** chosen for the study.

our own studies have indicated that the availability of an extra hydrogen bond donor at the C terminus can have dramatic influence on the folding profile of this class of compounds.[5a,6] Typically, three intramolecular hydrogen bonds that can stabilize 11-helical conformation are possible in **1** [Boc-C=O···NH(3), CO(1)···NH(4), and CO(2)···NH(5)], whereas **2**, having an additional NH at the C terminus, could accommodate four such bonds [Boc-C=O···NH(3), CO(1)···NH(4), CO(2)···NH(5), and

Table 1. Selected backbone torsions of hybrid peptides **1** and **2**.

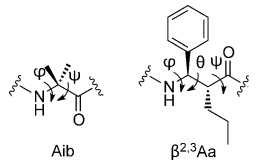

Peptide	Torsion angle	Residues Aib(1)	β^{2,3}-Aa (2)	Aib(3)	β^{2,3}-Aa (4)	Aib(5)
1[a]	ϕ	−57.9	−110.1	−55.5	−141.7	−56.4
	θ[b]	–	**85.9**	–	176.1	–
	ψ	−36.7	−73.5	−38.7	125.5	−50.2
2	ϕ	−60.9	−110.8	−57.0	−119.3	67.1
	θ[b]	–	**80.8**	–	171.4	–
	ψ	−30.7	−69.7	−40.4	134.8	28.6

[a] Data representative of one of the two isomorphs present in the unit cell. [b] Values in boldface indicate *gauche* conformational preference of these β residues.

[a] *Dr. D. Balamurugan, Dr. K. M. Muraleedharan*
Department of Chemistry
Indian Institute of Technology Madras, Chennai, 600036 (India)
E-mail: mkm@iitm.ac.in

Supporting information for this article is available on the WWW under http://dx.doi.org/10.1002/chem.201501198.

CO(3)···NH(Bn)]. However, folding will happen only if these interactions give impetus for a conformational shift from *anti* to *gauche* across C_α–C_β in one or both of β residues. Peptides **3** and **4** are the next higher oligomers, which can choose to exist either as a full-length helix or in a partially folded form, with lesser number of turns.

The hybrid peptide benzyl esters **1** and **3** and their benzyl amides **2** and **4** were prepared through solution-phase protocol and characterized by spectroscopic and mass spectrometric techniques (see the Supporting Information). Efforts to get information on their conformations in solid and solution states were then initiated. Out of various attempts, we succeeded in getting good quality crystals of **1** from a $CHCl_3$/*i*PrOH (1:1) solution for X-ray diffraction analysis.[7] As expected on the grounds of available hydrogen bonding interactions, it was found to adopt a partially folded structure, with the second β unit in *gauche* and the 4th β unit in *anti* conformation (Table 1 and Figure 2c). There were two hydrogen bonds, involving Boc-C=O···NH(3) and CO(1)···NH(4), which stabilized a 11-helix in the first half of the molecule with the remaining part extended, making it a hybrid of helix and strand! (Figure 2c and 2e). In fact, crystal structure of its next higher homologue with $(\alpha$–$\beta)_3$ composition, that was reported earlier (crystals grown from $CHCl_3$ solution) had all the four expected intramolecular H-bonds [Boc-C=O···NH(3), CO(1)···NH(4), CO(2)···NH(5), and CO(3)···NH(6)], which stabilized a 11-helical conformation.[5a] In comparison with this, the peptide **1** presented here is shorter by one β residue at the C terminus. This difference has, interestingly, caused partial unwinding, with the N-terminal region still holding the first two sets of H-bonds, which is noteworthy. To know the preference in the solution state, the ^{1}H NMR and ROESY spectra were analyzed simultaneously. Normally, information on C_α–C_β torsions in such systems (and, hence, an indirect information on local folding) can be obtained from $^3J_{C\alpha H-C\beta H}$. However, poor ^{1}H NMR resonance dispersion in $CDCl_3$ made analysis of the torsions as well as NOE interpretation difficult (Figure S9 in the Supporting Information). Interestingly, the spectrum recorded in [D_8]toluene/$CDCl_3$ mixture (4:1) had well resolved peaks. There were two clear doublets of doublets at $\delta = 5.28$ and 5.24 ppm, corresponding to 2nd and 4th C_βHs, respectively. *J* values of 4.0 and 5.5 Hz for their coupling with C_α protons indicated tendency to equilibrate to *gauche* rotameric states in these β residues. The ^{1}H NMR spectrum of its higher homologue **3** gave good dispersion when recorded in [D_8]toluene/$CDCl_3$ mixture (4:1) and had three clear doublets of doublets for C_βHs. $^3J_{C\alpha H-C\beta H}$ values for the C_βHs were in the range of 3.5–5.5 Hz, again indicative of their equilibration to *gauche* conformation in this solvent mixture. Although these indicated a drive towards folding in **1** and **3**, no supporting NOEs were seen in their ROESY spectra. Hence, the amide derivatives **2**

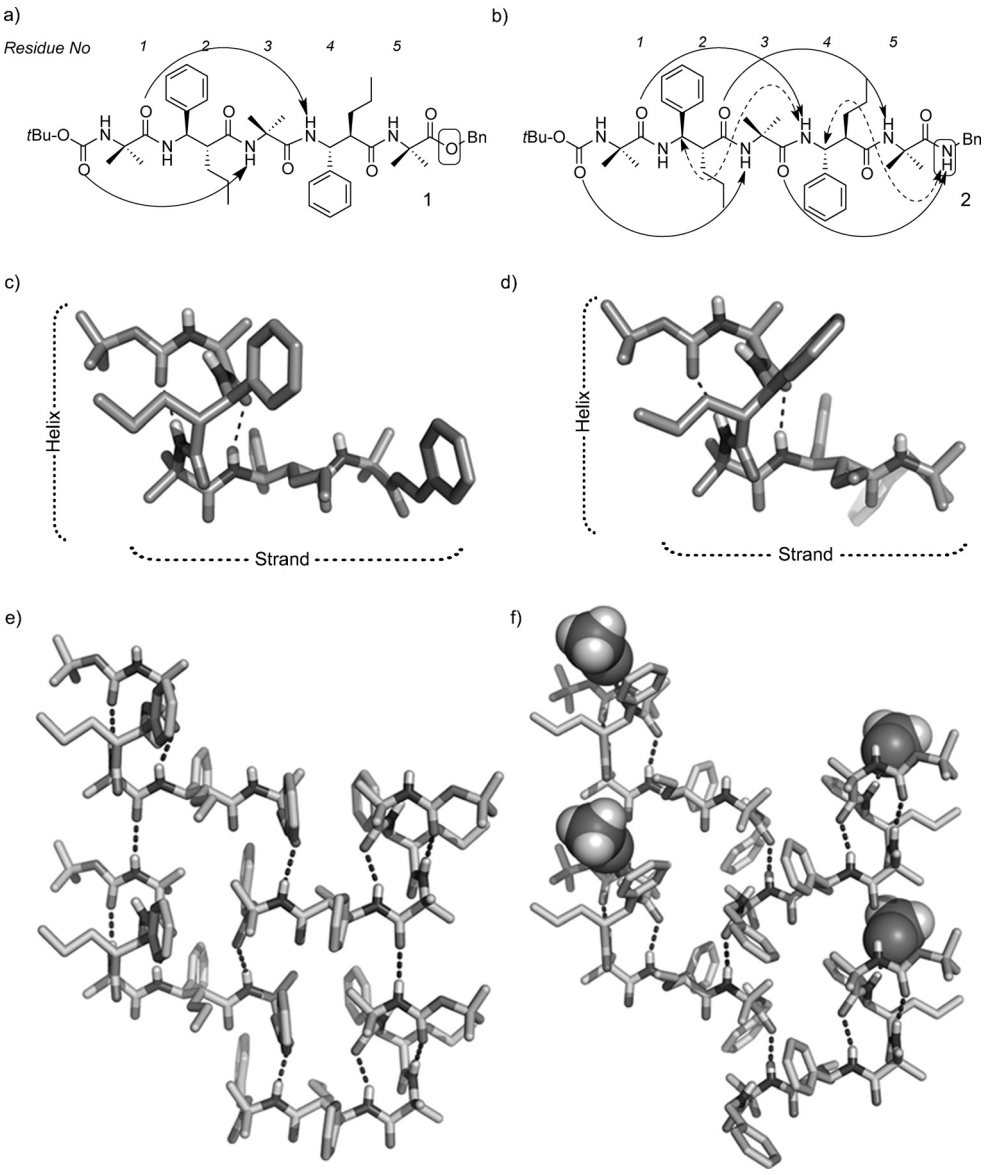

Figure 2. a–d) Chemical- and X-ray crystal structures of peptides **1** and **2**. Dotted arrow lines in b) show non-sequential *i*,*i*+2 NOEs in its ROESY ($CDCl_3$) spectrum. Solid arrow lines show intramolecular hydrogen bondings in the crystal structures. e) and f) Organization of molecules in the lattices of **1** and **2** respectively; H-bonding interactions are shown by dotted lines. Non-relevant hydrogen atoms have been removed for clarity. Co-crystallized methanol molecules in the crystal structure of **2** are shown as solid-spheres.

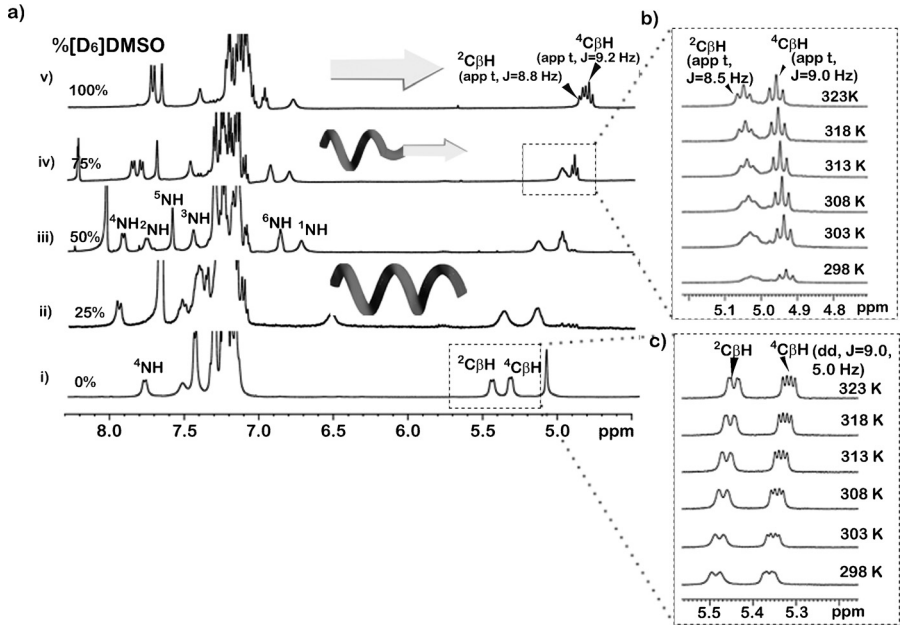

Figure 3. a) Relevant regions from the ^{1}H NMR spectra of pentapeptide benzylamide **2** recorded in varying proportions of [D_6]DMSO in $CDCl_3$ (i-v); percentage of [D_6]DMSO is indicated on the left hand side. Selected $C_\beta H$ regions showing the temperature effect on **2** in: b) 75% [D_6]DMSO/$CDCl_3$, and c) in 100% $CDCl_3$.

and **4**, which gave well-dispersed NMR spectra, were chosen for looking at partially folded structures and conformational transitions.

The ^{1}H NMR signals of **2** in $CDCl_3$ were well resolved and peak assignments were made using a combination of ^{1}H, COSY, TOCSY, and ROESY experiments (Figure 3 a(i)). Here, the 2nd $C_\beta H$ appeared as an apparent doublet at $\delta = 5.49$ ppm ($^3J_{C\alpha H-C\beta H}$ very small and $^3J_{NH-C\beta H}$ about 10.0 Hz), whereas the 4th $C_\beta H$ gave a clear doublet of doublet with J values of 3.5 and 9.5 Hz (Figure S3 in the Supporting Information). Appearance of these peaks suggested 2nd and 4th β residues as having *gauche* conformational preference. This, along with two long-range NOEs between $^2C_\beta H \rightarrow {}^4$NH and $^4C_\beta H \rightarrow {}^6$NH suggested 11-helical conformation in this solvent (Figure S12 in the Supporting Information).[8] This was anticipated, because this peptide (**2**) has all hydrogen bonding partners, as in the hexapeptide with $(\alpha-\beta)_3$ composition mentioned earlier.[5a] The fact that a hydrogen bonding solvent can cause partial unwinding and assist lattice assembly became clear when crystals obtained from a $CHCl_3$/MeOH (1:1) mixture were subjected to X-ray diffraction analysis.

Unlike the situation in $CDCl_3$, presence of methanol during crystallization of **2** led to partial unwinding of the helix to give the hybrid structure shown in Figure 2 d; there were two intramolecular [Boc(C=O)···HN(3) and C=O(1)···HN(4)] hydrogen bonds as seen in the solid-state structure of **1**. But the lattice of **2** was distinguished by the presence of methanol as part of the lattice, establishing hydrogen bonding to ^{2}NH of each molecule, as shown in Figure 2 f. This lattice-bound MeOH may not be the sole contributor of partial unwinding, and many such interactions in the C-terminal region might have given way for intermolecular CO···HN hydrogen bonding during nucleation and lattice development. Since our attempts to crystallize **1** and **2** from $CHCl_3$ were not fruitful, a direct comparison of their solid-state structures with that of hexapeptide homologue[5a] could not be made: Nevertheless, the observed difference is attributable to the difference in the chemical environment during crystallization. Important crystallographic data of **1** and **2** are presented in Table 2.

Supramolecular organizations of peptide helices and strands individually are abundant in literature.[1e,9] Having a hybrid of these two conformations, **1** and **2** appeared useful to understand new preferences, hitherto unseen. Analysis of their lattices showed two intermolecular hydrogen bonds in each case [C=O(3)···HN(1) and C=O(5)···HN(5)], apart from the intramolecular hydrogen bonds mentioned above. Of these, the C=O(3)···HN(1) interaction was between molecules arranged one above the other, which aligned the helical parts vertically, whereas C=O(5)···HN(5) interaction was between molecules positioned horizontally, and gave a sheet-like arrangement typical of β strands (Figure 2 e, f). Such a combination of extreme conformations in a single lattice, with supramolecular arrangement through segregation of helical and extended regions, is exceptional and probably the first of its kind.

Table 2. Hydrogen bond lengths and angles in the crystal structures of peptides **1** and **2**.

Peptide	Type		H···O [Å]	N···O [Å]	∢N-H···O [°]
1	Boc(C=O)···HN(3)	intra	2.197	3.035	164.78
	C=O(1)···HN(4)		2.172	2.962	152.61
	C=O(3)···HN(1)	inter	2.138	2.969	162.13
	C=O(5)···HN(5)		2.275	3.038	147.89
2	Boc(C=O)···HN(3)	intra	2.200	3.033	163.18
	C=O(1)···HN(4)		2.085	2.919	163.35
	C=O(3)···HN(1)	inter	2.121	2.979	175.74
	C=O(5)···HN(5)		2.044	2.886	166.08

With these preliminary results, we set out to look at the presence of partially unfolded structures of these peptides in $CDCl_3$, by using [D_6]DMSO as the co-solvent. DMSO titration is a standard procedure to locate the solvent-exposed NHs. By using the same logic, we envisaged that partial unfolding in the presence of this solvent, if at all, will happen in such way that more labile hydrogen bond(s) are disrupted first, which can be monitored by looking at $^3J_{C\alpha H-C\beta H}$ values as well as NOEs along the backbone.

The ^{1}H NMR spectrum of peptide **2** in 50% [D$_6$]DMSO/CDCl$_3$ had a well-dispersed amide region along with two broad peaks for their C$_\beta$ hydrogens (Figure 3a(iii)). ROESY experiment at this [D$_6$]DMSO concentration had two long range NOEs (^{2}C$_\beta$H→^{4}NH and ^{4}C$_\beta$H→^{6}NH) as in the spectrum recorded in CDCl$_3$ (Figure S24 in the Supporting Information). Further increase in [D$_6$]DMSO content to 75% changed the ^{4}C$_\beta$H splitting into apparent triplet with equal *J* values of 9.2 Hz for their couplings with C$_\alpha$H and NH peaks. This indicated the *anti* conformational preference of 4th C$_\beta$ unit and an extended structure in the second half of the molecule. At the same time, 2nd C$_\beta$H signal remained broad. Whereas this suggested conformational exchange between the *gauche* and the *anti* forms in the second residue, the ROESY spectrum recorded in this solvent composition (75% [D$_6$]DMSO, Figure 4) had the long range ^{2}C$_\beta$H→^{4}NH NOE in support of a preference for 11-helical conformation in the first half.[8] Thus, the partially unfolded conformation that was seen in the solid state seems to also exist in solution on appropriate solvation. Further increase in the [D$_6$]DMSO concentration to 100% caused complete disruption of all the H-bonds, resulting in an extended structure, which is evidenced by large $^{3}J_{C\alpha H-C\beta H}$ values of second and fourth β residues, and disappearance of NOEs between ^{2}C$_\beta$H→^{4}NH and ^{4}C$_\beta$H→^{6}NH.

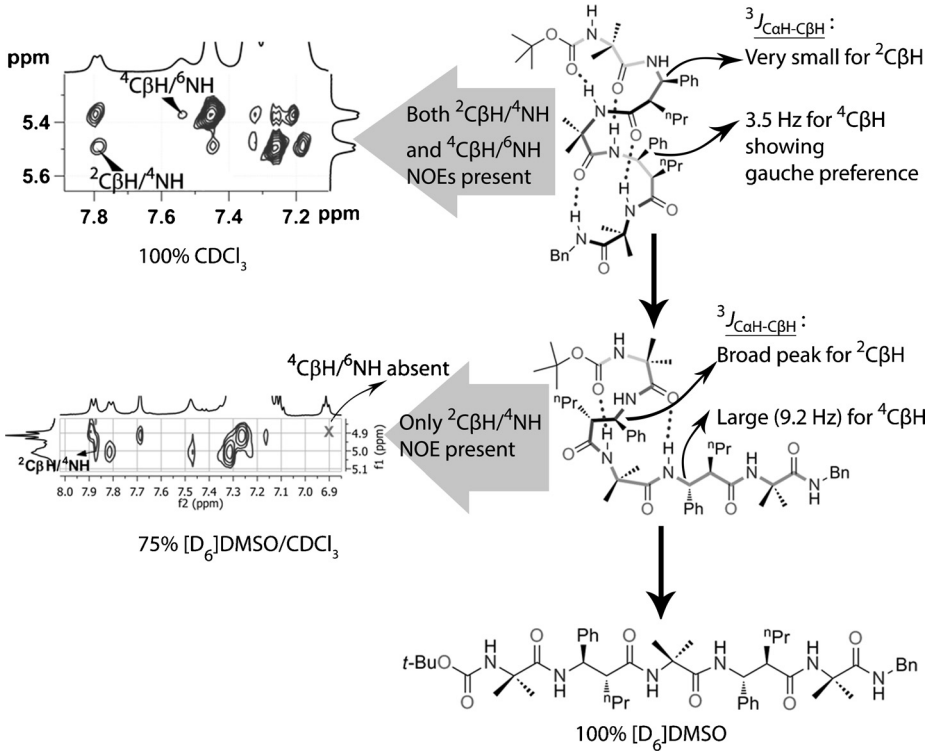

Figure 4. Relevant regions from ROESY spectra of **2** recorded in 100% CDCl$_3$ and 75% [D$_6$]DMSO/CDCl$_3$ suggestive of 'step-wise' unwinding; variation in $^{3}J_{C\alpha H-C\beta H}$ values of 2nd and 4th β residues are also shown.

At this stage, it was important to see whether a small temperature jump can change the partially folded state of sample in 75% [D$_6$]DMSO/CDCl$_3$ to a completely extended structure. Towards this, a variable temperature (VT) NMR study between 298 and 328 K was carried out. As evident from Figure 3b, the splitting pattern of ^{2}C$_\beta$H became more refined and changed to *apparent triplet* with equal *J* value for C$_\alpha$H–C$_\beta$H and C$_\beta$H–NH couplings (8.5 Hz) on increasing the temperature to 323 K. During this, the signal for ^{4}C$_\beta$H remained intact, suggesting that the transition happens mainly in the first half of the molecule (Figure 3b). When a similar experiment was done for a sample in 100% CDCl$_3$, we could see a refinement of splitting pattern without any significant change in $^{3}J_{C\beta H-C\alpha H}$ values, showing better stability of 11-helical structure under this condition (Figure 3c).

The ^{1}H NMR signals of the higher homologue **4** (Figure 5) recorded in CDCl$_3$ were also well resolved. Its 2nd, 4th, and 6th C$_\beta$H signals appeared at $\delta = 5.55$, 5.65, and 5.45 ppm, respectively, as apparent doublets with *J* values of 10.0, 10.0, and 9.0 Hz (for $^{3}J_{NH}$), respectively. This suggests that their coupling constants with the adjacent C$_\alpha$Hs ($^{3}J_{C\beta H-C\alpha H}$) are small (Figure 6a(i)), which indicates their *gauche* conformational preference. The ROESY spectrum recorded in CDCl$_3$ showed three non-sequential *i*,*i*+2 NOEs (^{2}C$_\beta$H→^{4}NH, ^{4}C$_\beta$H→^{6}NH and ^{6}C$_\beta$H→^{8}NH), characteristic of 11-helical structure (Figure 5). Attempts to get good quality crystals of this compound for X-ray diffraction analysis were not fruitful.

This peptide (**4**), having three pairs of intramolecular hydrogen bonding, seemed ideal to delve deeper in to the process of stepwise unwinding. If such a process really happens, each of the long range NOEs, ^{2}C$_\beta$H→^{4}NH, ^{4}C$_\beta$H→^{6}NH, and ^{6}C$_\beta$H→^{8}NH, should disappear one by one on increasing the [D$_6$]DMSO content; this should also be accompanied by a concomitant change in the splitting pattern and $^{3}J_{C\alpha H-C\beta H}$ values of C$_\beta$Hs from one end to the other.

Changes in C$_\beta$H signal splitting pattern on increasing [D$_6$]DMSO

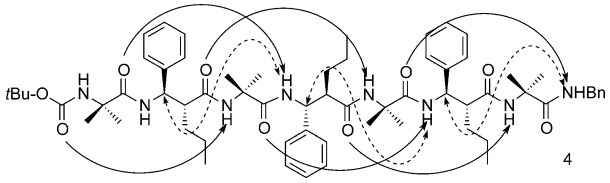

Figure 5. Chemical structure of peptide **4**. Dotted arrow lines show non-sequential *i*,*i*+2 NOEs in its ROESY spectrum recorded in CDCl$_3$. Intramolecular hydrogen bonds proposed based on NMR data are shown by solid arrow lines.

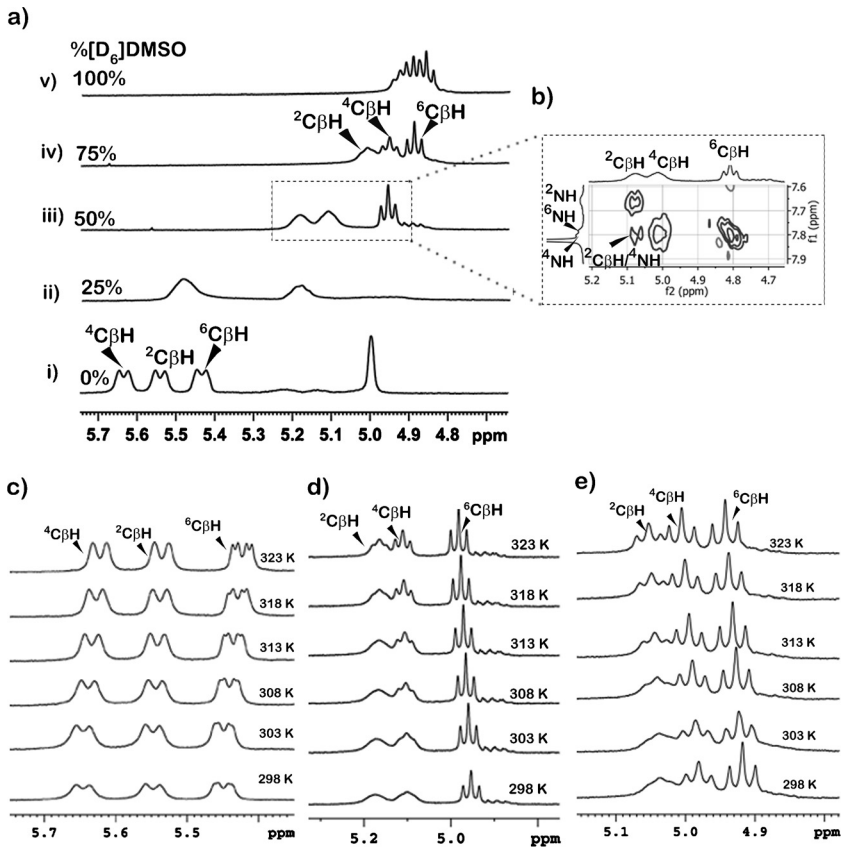

Figure 6. a) Relevant regions from the ^{1}H NMR spectra of hepta peptide- benzylamide **4** recorded in varying proportions of [D_6]DMSO in $CDCl_3$ (i–v); percentage of [D_6]DMSO is indicated on the left hand side. b) Expanded region of ROESY spectrum recorded in 50% [D_6]DMSO/$CDCl_3$ showing $^{2}C_\beta H \rightarrow {}^{4}NH$ NOE; Selected $C_\beta H$ regions showing the temperature effect on **4** in c) 100% $CDCl_3$, d) 50% [D_6]DMSO/$CDCl_3$ and, e) 75% [D_6]DMSO/$CDCl_3$.

content from 0 to 100% and the effect of temperature are shown in Figure 6. As evident from Figure 6c, the apparent doublets observed for all $C_\beta Hs$ in $CDCl_3$ and their $^{3}J_{C\alpha H-C\beta H}$ values remained largely unaffected on increasing the temperature from 298 to 323 K, showing good helical preference along the entire backbone. Although the dispersion of the NMR signals was poor at 25% [D_6]DMSO, there was improvement on increasing it to 50%. Notably, the $^{6}C_\beta H$ signal changed its splitting to apparent triplet at this concentration, whereas those for $^{2}C_\beta H$ and $^{4}C_\beta H$ were broad. This suggest *anti* conformation across C_α–C_β in the former and some degree of equilibration between *gauche* and *anti* forms in the latter two residues. Remarkably, the $^{2}C_\beta H \rightarrow {}^{4}NH$ NOE was still present in the ROESY spectrum, pointing towards helical preference in the N-terminal region (Figure 6b).[8] Since there was only $\delta =$ 0.02 ppm difference in the chemical shifts of ^{4}NH and ^{6}NH signals, the NOE between $^{4}C_\beta H \rightarrow {}^{6}NH$ was difficult to distinguish (Figure 6b). As expected, based on the splitting of $^{6}C_\beta H$ signal, the NOE between $^{6}C_\beta H \rightarrow {}^{8}NH$ was absent, suggesting an extended C-terminal region. Figure 6d shows the effect of temperature on the splitting pattern of $C_\beta H$ signals at this [D_6]DMSO concentration (50%). The 2nd and 4th $C_\beta H$ signals, which were broad, became more refined and emerged as apparent triplets on rising the temperature to 323 K, suggesting a shift towards *anti* conformation in these residues and complete unfolding. Overall, use of 50% [D_6]DMSO has caused the peptide to unwind in the C terminus, with the N-terminal region equilibrating more towards helical form due to larger proportion of *gauche* rotameric states in 2nd β residue. Increasing the [D_6]DMSO content to 75% could give a similar effect, and the outcome is presented in Figure 6a(iv). Here, both 4th and 6th $C_\beta Hs$ were apparent triplets, showing extended conformation in that segment, whereas the $2C_\beta H$ signal was broad. As in the previous case, increasing temperature caused this also to transform to apparent triplet as shown in Figure 6e.

Nucleation of secondary structures, directed through specific sets of intramolecular secondary interactions and facilitated by appropriate backbone/side-chain torsions, is central to protein folding process.[4b,10] The guiding principles involved seem to be applicable to oligomers from synthetic amino acids as well.[5e,11] Although both secondary and super-secondary structures based on peptides from β- and γ-amino acids have been reported,[1k,l] such synthetic systems have rarely been used for understanding the folding/unfolding pathways. Previous observations in this area include: the existence of partially folded structure in oligocarbamate foldamers belonging to γ-peptide superfamily,[12] zig-zag tape-like structures in the hybrid foldamer of leucine with 8-amino-2-quinolinecarboxylic acid,[13] inversion of helix handedness in aromatic oligoamide foldamers based on 8-amino-2-quinoline carboxylic acid,[14] 'non-cooperative' unfolding in β-peptide foldamers reported by Gademann et al.,[15] accessibility of both 10- and 14-helical conformations in trans-2-amino-cyclohexanecarboxylic acid-based foldamers[16] and $\alpha/3_{10}$-helix dimorphism in N_α-acylated heptapeptide amide, Ac-[L-(αMe)Val]$_7$-NH*i*Pr which contain C_α-methyl-L-valine as the building block.[17] The details presented in this manuscript are part of our efforts along similar lines. Among the benzyl esters and amides, NMR signal dispersion was better in the latter and, hence, they were chosen for monitoring the unfolding process upon changing the solvent polarity and/or increasing temperature. Since the splitting pattern of $C_\beta H$ signal was diagnostic of the θ torsion of that residue, it was possible to get information on the extent of unfolding by looking at this signal from different β residues. On increasing the solvent polarity, each of the

$C_\beta H$ signal was found to change from apparent doublet to apparent triplet indicating *gauche*-to-*anti* shift in a systematic manner. Increased population of partially folded conformations was also seen, which is indicated by the relevant NOEs in their ROESY spectrum.

A comparison of the conformational preferences of peptides presented here with those of $\alpha,\beta^{2,3}$-hybrid peptides with $(\alpha\text{–}\beta)_n$ composition reported previously is also important. The tetra-, hexa-, and octa-peptides belonging to the latter group had shown good tendency to adopt 11-helical structures; all their internal β residues were found to adopt *gauche* conformation across C_α–C_β to facilitate intramolecular hydrogen bonding, leaving the terminal one in *anti* conformation.[5a] The drive to undergo anti to *gauche* shift in response to hydrogen bonding was evident from the conformations of tripeptide benzyl ester (strand) and the corresponding benzylamide (11-helix) in the same series. The present work has taken the study to the next level and has shown that higher homologues with $(\alpha\text{–}\beta)_n\alpha$ composition, though largely helical in $CDCl_3$ solution, can exist in partially unfolded conformation on appropriate solvation and/or rise in temperature. More importantly, it was possible to execute the transition from a folded- to completely unfolded state in a systematic manner through stepwise *gauche*-to-*anti* shift of C_α–C_β torsions in β residues from C to N terminus, which manifested as sequential unfolding of helical turns.

To summarize, the present study involving trans-$\beta^{2,3}$-hybrid peptides gives a closer look at folding/unfolding process in response to variation in solvent polarity and temperature. X-ray crystallography and NMR spectroscopy of penta- and hepta-peptide C-terminal amides from this series show that specific sets of hydrogen bonds, stabilizing each of the helical folds, can be disrupted in a sequential manner through incremental variation in solvent polarity and/or temperature. In $CDCl_3$, these peptides have an 11-helical conformation, but increase of $[D_6]$DMSO content from 0–100% caused a concomitant disruption of hydrogen bonds from C-to N-terminal region, leading to gradual unwinding of the helical structure. The partially folded intermediate conformations seem to have extended C-terminal region, whereas the β residues located towards the N terminus showed greater tendency to adopt gauche conformation and retain *i*,*i*+3 C=O···HN intramolecular H-bonds.

Acknowledgements

Financial support of this work by the Department of Science and Technology, INDIA (Grants SR/S1/OC-13/2007), instrumentation facility by IIT Madras, and DST-FIST (New Delhi) are gratefully acknowledged. We thank Mr. V. Ramkumar, Department of Chemistry for X-ray diffraction analysis. D. Balamurugan thanks DST and IITM for the research fellowship.

Keywords: alpha/beta-hybrid peptides · amino acids · foldamers · helix-strand hybrid · protein folding

[1] a) D. H. Appella, L. A. Christianson, I. L. Karle, D. R. Powell, S. H. Gellman, *J. Am. Chem. Soc.* **1996**, *118*, 13071; b) S. Krauthäuser, L. A. Christianson, D. R. Powell, S. H. Gellman, *J. Am. Chem. Soc.* **1997**, *119*, 11719; c) D. Seebach, S. Abele, K. Gademann, G. Guichard, T. Hintermann, B. Jaun, J. L. Matthews, J. V. Schreiber, L. Oberer, U. Hommel, H. Widmer, *Helv. Chim. Acta* **1998**, *81*, 932; d) S. Hanessian, X. Luo, R. Schaum, S. Michnick, *J. Am. Chem. Soc.* **1998**, *120*, 8569; e) D. Seebach, S. Abele, K. Gademann, B. Jaun, *Angew. Chem. Int. Ed.* **1999**, *38*, 1595–1597; *Angew. Chem.* **1999**, *111*, 1700–1703; f) R. P. Cheng, S. H. Gellman, W. F. DeGrado, *Chem. Rev.* **2001**, *101*, 3219; g) X. Daura, K. Gademann, H. Schaefer, B. Jaun, D. Seebach, W. F. van Gunsteren, *J. Am. Chem. Soc.* **2001**, *123*, 2393; h) D. Seebach, M. Brenner, M. Rueping, B. Schweizer, B. Jaun, *Chem. Commun.* **2001**, 207; i) D. Seebach, M. Brenner, M. Rueping, B. Jaun, *Chem. Eur. J.* **2002**, *8*, 573; j) T. A. Martinek, F. Fülöp, *Eur. J. Biochem.* **2003**, *270*, 3657; k) D. Seebach, A. K. Beck, D. J. Bierbaum, *Chem. Biodiversity* **2004**, *1*, 1111; l) P. G. Vasudev, S. Chatterjee, N. Shamala, P. Balaram, *Chem. Rev.* **2011**, *111*, 657.

[2] a) M. A. Schmitt, B. Weisblum, S. H. Gellman, *J. Am. Chem. Soc.* **2004**, *126*, 6848; b) D. F. Hook, P. Bindschädler, Y. R. Mahajan, R. Šebesta, P. Kast, D. Seebach, *Chem. Biodiversity* **2005**, *2*, 591; c) M. A. Schmitt, B. Weisblum, S. H. Gellman, *J. Am. Chem. Soc.* **2007**, *129*, 417; d) J. D. Sadowsky, W. D. Fairlie, E. B. Hadley, H.-S. Lee, N. Umezawa, Z. Nikolovska-Coleska, S. Wang, D. C. S. Huang, Y. Tomita, S. H. Gellman, *J. Am. Chem. Soc.* **2007**, *129*, 139; e) W. S. Horne, S. H. Gellman, *Acc. Chem. Res.* **2008**, *41*, 1399; f) W. S. Horne, L. M. Johnson, T. J. Ketas, P. J. Klasse, M. Lu, J. P. Moore, S. H. Gellmana, *Proc. Natl. Acad. Sci. USA* **2009**, *106*, 14751; g) L. K. A. Pilsl, O. Reiser, *Amino Acids* **2011**, *41*, 709.

[3] a) D. H. Appella, L. A. Christianson, D. A. Klein, M. R. Richards, D. R. Powell, S. H. Gellman, *J. Am. Chem. Soc.* **1999**, *121*, 7574; b) Y. J. Chung, B. R. Huck, L. A. Christianson, H. E. Stanger, S. Krauthauser, D. R. Powell, S. H. Gellman, *J. Am. Chem. Soc.* **2000**, *122*, 3995; c) S. H. Choi, I. A. Guzei, L. C. Spencer, S. H. Gellman, *J. Am. Chem. Soc.* **2008**, *130*, 6544.

[4] a) G. D. Rose, P. J. Fleming, J. R. Banavar, A. Maritan, *Proc. Natl. Acad. Sci. USA* **2006**, *103*, 16623; b) R. L. Baldwin, *J. Mol. Biol.* **2007**, *371*, 283.

[5] a) D. Balamurugan, K. M. Muraleedharan, *Chem. Eur. J.* **2012**, *18*, 9516; b) B. V. Venkataram Prasad, P. Balaram, *CRC Crit. Rev. Biochem.* **1984**, *16*, 307; c) I. L. Karle, P. Balaram, *Biochemistry* **1990**, *29*, 6747; d) C. Toniolo, E. Benedetti, *Macromolecules* **1991**, *24*, 4004; e) J. Venkatraman, S. C. Shankaramma, P. Balaram, *Chem. Rev.* **2001**, *101*, 3131.

[6] a) P. Maity, M. Zabel, B. König, *J. Org. Chem.* **2007**, *72*, 8046; b) S. H. Choi, I. A. Guzei, S. H. Gellman, *J. Am. Chem. Soc.* **2007**, *129*, 13780; c) A. Bandyopadhyay, H. N. Gopi, *Org. Lett.* **2012**, *14*, 2770.

[7] There were two isomorphs in the unit cell of **1**. Both had their 2nd β residue in *gauche* and the 4th β residue in *anti* conformations, and had overall 'helix-strand hybrid' conformation. Crystal data for **1**: from $CHCl_3$/*i*PrOH, $C_{48}H_{67}N_5O_8$; $M_r = 842.07$; crystal size $0.35\times0.20\times0.15$ mm; colorless needles; monoclinic; space group $P2_1$; $a = 21.291(9)$, $b = 10.585(3)$, $c = 23.222(7)$ Å; $\alpha = 90$, $\beta = 90.059(14)$, $\gamma = 90^\circ$; $V = 5233(3)$ Å^3; $Z = 4$, $T = 298$ K; $Mo_{K\alpha} = 0.71073$; $0.88 < \theta < 26.53$, 13928 reflections measured; 9079 unique reflections; $R1 = 0.1100$ and $wR2 = 0.2408$; GOF = 1.21; Crystal data for **2**: from $CHCl_3$/MeOH, $C_{49}H_{71}N_6O_8$; $M_r = 872.12$; $0.25\times0.20\times0.15$ mm; colorless needles; orthorhombic; space group $P2_12_12_1$; $a = 10.4792(6)$, $b = 20.2449(12)$, $c = 25.0931(6)$ Å; $\alpha = 90$, $\beta = 90$, $\gamma = 90^\circ$; $V = 5323.5(6)$ Å^3; $Z = 4$; $T = 298$ K; $Mo_{K\alpha} = 0.71073$; $1.91 < \theta < 17.55$; 8188 reflections measured; 3387 unique reflections; $R1 = 0.0508$ and $wR2 = 0.1293$; GOF = 0.981. CCDC-945944 (**1**) and CCDC-945945 (**2**) contain the supplementary crystallographic data for this paper. These data can be obtained free of charge from The Cambridge Crystallographic Data Centre via www.ccdc.cam.ac.uk/data_request/cif.

[8] The non-sequential NOEs observed in the present study were either in the medium or weak range.

[9] a) D. H. Appella, L. A. Christianson, I. L. Karle, D. R. Powell, S. H. Gellman, *J. Am. Chem. Soc.* **1999**, *121*, 6206; b) J. S. Nowick, *Acc. Chem. Res.* **2008**, *41*, 1319.

[10] a) J. K. Myers, T. G. Oas, *Nat. Struct. Biol.* **2001**, *8*, 552; b) S. E. Miller, A. M. Watkins, N. R. Kallenbach, P. S. Arora, *Proc. Natl. Acad. Sci. USA* **2014**, *111*, 6636.

[11] T. A. Martinek, F. Fülöp, *Chem. Soc. Rev.* **2012**, *41*, 687.

[12] Y. R. Nelli, L. Fischer, G. W. Collie, B. Kauffmann, G. Guichard, *Biopolymers* **2013**, *100*, 687.

[13] M. Kudo, V. Maurizot, H. Masu, A. Tanatani, I. Huc, *Chem. Commun.* **2014**, *50*, 10090.

[14] N. Delsuc, T. Kawanami, J. Lefeuvre, A. Shundo, H. Ihara, M. Takafuji, I. Huc, *ChemPhysChem* **2008**, *9*, 1882.
[15] K. Gademann, B. Jaun, D. Seebach, R. Perozzo, L. Scapozza, G. Folkers, *Helv. Chim. Acta* **1999**, *82*, 1.
[16] A. Hetényi, I. M. Mandity, T. A. Martinek, G. K. Toth, F. Fueloep, *J. Am. Chem. Soc.* **2005**, *127*, 547.
[17] M. Crisma, M. Saviano, A. Moretto, Q. B. Broxterman, B. Kaptein, C. Toniolo, *J. Am. Chem. Soc.* **2007**, *129*, 15471.

Received: March 26, 2015
Published online on May 15, 2015